

Intelligent Icing Detection Model of Wind Turbine Blades Based on SCADA data

Wenqian Jiang, Junyang Jin

Abstract—Diagnosis of ice accretion on wind turbine blades is all the time a hard nut to crack in condition monitoring of wind farms. Existing methods focus on mechanism analysis of icing process, deviation degree analysis of feature engineering. However, there have not been deep researches of neural networks applied in this field at present. Supervisory control and data acquisition (SCADA) makes it possible to train networks through continuously providing not only operation parameters and performance parameters of wind turbines but also environmental parameters and operation modes. This paper explores the possibility that using convolutional neural networks (CNNs), generative adversarial networks (GANs) and domain adaption learning to establish intelligent diagnosis frameworks under different training scenarios. Specifically, PGANC and PGANT are proposed for sufficient and non-sufficient target wind turbine labeled data, respectively. The basic idea is that we consider a two-stage training with parallel GANs, which are aimed at capturing intrinsic features for normal and icing samples, followed by classification CNN or domain adaption module in various training cases. Model validation on three wind turbine SCADA data shows that two-stage training can effectively improve the model performance. Besides, if there is no sufficient labeled data for a target turbine, which is an extremely common phenomenon in real industrial practices, the addition of domain adaption learning makes the trained model show better performance. Overall, our proposed intelligent diagnosis frameworks can achieve more accurate detection on the same wind turbine and more generalized capability on a new wind turbine, compared with other machine learning models and conventional CNNs.

I. INTRODUCTION

Global warming is one of the most powerful actors for promoting renewable sources a promising alternative to traditional fossil fuels, of which wind energy has received increasing attention. As “the fastest growing renewable energy source in the world” with an average annual growth of 30% over the past two decades [16], wind power has grown to an essential part to achieve emission reduction targets in the future. The GlobalWind Energy Council makes a prediction that the installed capacity global wind power is expected to increase to 840 GW by the end of 2022.

Any renewable Energy requires the advances in the reliability, availability, maintainability and safety in order to be competitive in the electrical energy market [46], wind power is no exception. Wind power generation often faces some challenges that restrict its development, such as blades icing monitoring studied in our paper. Wind farms are mostly located on high altitude mountainous areas, making their

operating conditions under low temperature and high humidity. Therefore, the phenomenon of wind turbine blades icing is almost unavoidable, especially in winter. Any wind turbine blade icing will have the possibility to cause loss of power generation, mechanical and equipment failure, and potential safety hazards [12].

Various signals acquired by the monitoring technology and sensors can be utilized to distinguish the icing turbines. For example, a monitoring camera can be installed on the wind turbine [18], and then researchers apply hyperspectral imaging technology to find icing wind turbine blades [29]. Vibration signal analysis such as using changes in natural frequencies can contribute to detect damage for blades[41]. Besides, the Supervisory Control and Data Acquisition (SCADA) is a strong system for data acquisition and equipment monitoring, which is also the most widely used and technologically advanced in fault diagnosis of a large amount of wind power elements[35], [9], [10]. From SCADA, not only the operating parameters of wind power equipment, but also environmental parameters such as temperature, are collected, both of which give a full description of the status of wind turbines. More and more researchers use it for data modeling and analysis to mine information of equipment fault and blade icing detection, etc. [10], [6].

The International Electro technical Commission (IEC) has developed many standards and guidelines to help analyze turbine faults[1]. Physical model of icing and theoretical analysis is mainly considered in the existing methods. Battisti et al give a detailed description about the causes and types of blade icing and analyze the effect of icing process on wind turbines in [5]. Lichun et al study the relationship between the icing positions on wind turbines and output power in [33]. Han et al focus on the freezing condition under different temperature, liquid water content and wind speed in [17]. Dong et al utilize the deviation degree of output power performance, mechanical performance and aerodynamic performance characteristic parameters in blades icing timing to establish blades icing identification model based on SCADA data [11].

Data-driven models have shown promising performance in exploring the relationship between the operation variables and the icing, recently. Li et al. proposed a method for identification of icing blades based on logistic regression [27]. Skrimpas et al. combine vibration and power curve analysis with the K-Nearest Neighbours (KNN) method for icing turbines detection [34]. Zhang et al propose a blade icing prediction model based on Random Forest Classifier [44]. Yuan et al put forward a deep time series classification model called WaveletFCNN for wind turbine blade icing detection

Wenqian Jiang is with China-EU Institute for Clean and Renewable Energy, Huazhong University of Science and Technology, Wuhan, China, 430074.

Junyang Jin is with HUST-Wuxi Research Institute, Wuxi, China, 214000.

[43].

To the best of our known, only a few papers related to the neural networks have been proposed, there are still more work need to be done. Our paper proposes two neural networks, PGANC and PGANT, based on Generative Adversarial Networks (GAN) and transfer learning to help identify icing blades in wind farms using SCADA data. We firstly establish PGANC: two parallel GANs followed by a convolutional neural network (CNN). Through a two-stage training, it can achieve good performance on a single turbine. But when we test the trained PGANC model on a different wind turbine, the performance is not so satisfactory. Specifically, the identification of normal wind turbines is easier than that of icing cases. This is true because different wind turbines often operate under various environments and load conditions together with different physical characteristics, which means that the icing conditions are different from turbine to turbine. In addition, labeling the icing data from normal data is always time-consuming and labor-intensive. Therefore, we improve PGANC to PGANT: two parallel GANs followed by a transfer learning framework to deal with the above problem. This paper makes the following contributions:

- 1) Two intelligent icing diagnosis frameworks: PGANC and PGANT are proposed for various training scenarios. For the same wind turbine with sufficient labeled data, PGANC shows better performance on the imbalanced SCADA data, where the number of icing samples is much less than that of normal samples. For a new wind turbine without sufficient labeled data, PGANT adopts domain adaption module to transfer the trained invariant features of another historical wind turbine.
- 2) A two-stage training process is taken into consideration. In both PGANC and PGANT, we first train GANs and CNNs or GANs and transfer framework in separate series way. After acquiring the optimal parameters, based on which the second holistically training can improve the performance further and reduce computing time.
- 3) Extensive experiments have been conducted to validate the effectiveness of our proposed methods. In PGANC, three wind turbine SCADA data is used. The results show that PGANC outperforms conventional CNNs, and the two-stage training is effective. Performance on 3 different transfer scenarios proves that PGANT can achieve more generalize capability.

This paper is organized as follows. Section II reviews related works including CNN and GAN for fault diagnosis and transfer learning. Section III proposes our two intelligent icing diagnosis frameworks. Experiment results and comparison are given in Section IV. Finally, conclusion and future work are drawn in Section V.

II. RELATED WORKS

In recent years, CNNs have long been popular in deep learning [38], [32], [28]. The initial CNN architecture was proposed by LeCun et al. in works [22] and [23], of which main features are local connections, shared weights, and local pooling [30]. They have been widely used in classification

tasks. For example, a 1-D convolutional neural network-based approach [7] has been proposed by Chen et al. to diagnose both known and unknown faults in rotating machinery under added noise. Gao et al. [13] developed a semi-supervised learning method based on CNN for steel surface defect recognition. [24] proposed a dislocated time series convolutional neural network called DTS-CNN to dislocate the 1D input mechanical signal into an output matrix.

In addition to CNNs, GANs occupy an increasingly pivotal position in the deep learning community. They were initially introduced by Goodfellow *et al.* as an unsupervised machine learning method [14]. The basic idea of GANs is that it generates prototypical samples through a generator with random data points that satisfy a certain distribution (e.g: Gaussian distribution). GANs are well known by the great power of feature extraction and pattern recognition [42], [45], [39]. In addition, GANs present outstanding performance in dealing with imbalanced datasets [40], which is especially demanding to handle the relatively minor icing cases in our paper. Various adversarial algorithms have been developed to construct GANs. GANs were applied to tackle imbalanced fault classification problems of machinery [37]. For more details, interested readers may refer to [3] for a comprehensive discussion of GANs and their variants.

Through transferring the knowledge from source domain to target domain under diverse operating conditions, transfer learning is often regarded as an efficient tool to solve the diagnostic or predictive tasks of unlabeled or insufficient data. We adopt the definition of transfer learning in [8]:

Transfer learning is proposed with the aim to learn a prediction function $\mathcal{F}(x) : x \rightarrow y$ for a learning task \mathcal{T}_t by leveraging knowledge from source domain \mathcal{D}_s and \mathcal{T}_s , where $\mathcal{D}_s \neq \mathcal{D}_t$ or $\mathcal{T}_s \neq \mathcal{T}_t$. In most of the cases, \mathcal{D}_s contains a much larger dataset than \mathcal{D}_t .

How to measure the distribution similarity between source domain and target domain is of vital importance in transfer learning. MMD is the most common seen distance measure used in existing transfer networks [25], [15], [31]. The MMD metric is a special case of the integral probability metrics which measures the distance between two probability distributions via mapping the samples into a Reproducing Kernel Hilbert Space associated with a given kernel.

III. WIND TURBINE BLADE ICING DETECTION USING DEEP LEARNING

A. PGANC: sufficient labeled data scenario

1) *Method overview:* For the same turbine with sufficient labeled data, the training process is supervised. Our neural network designed to classify states of wind turbine blades is as follows:

$$Y = NN(x) \quad (1)$$

where $x \in \mathcal{R}^{1 \times 28}$ is a vector containing 28 variables, $Y \in \mathcal{R}^{1 \times 2}$ is the output of the network indicating the probability of normal and icing state, and $NN(\cdot)$ is the neural network described by a composition of nonlinear functions that maps inputs to outputs.

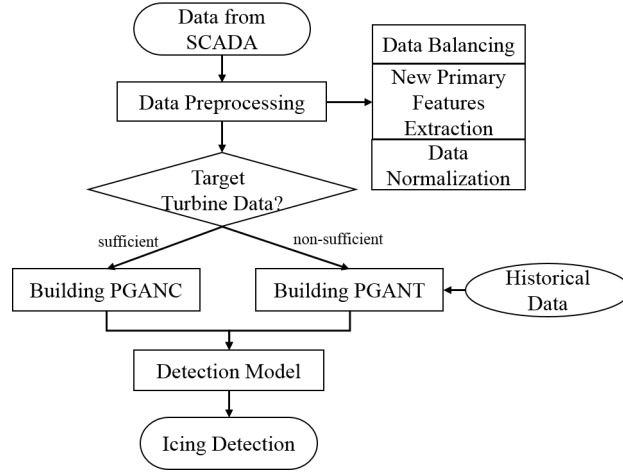


Fig. 1. Flow chart of model construction

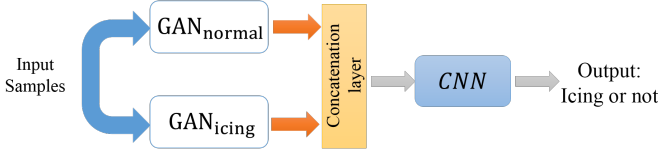


Fig. 2. GAN+CNN Framework

PGANC is composed of two GANs in parallel following by a CNN classifier as shown in Fig 2. As an unsupervised learning technique, GANs are powerful in extracting hidden features from inputs and capturing inherent patterns for target classes. CNNs are capable of learning spatial information among different dimensions and across multiple channels of inputs [20]. By combining GANs and CNNs, the derived neural network can efficiently conduct feature extraction and thus accurately perform classification.

A GAN consists of a generator $G(\cdot)$ and a discriminator $D(\cdot)$. The generator transform input samples into synthetic ones in order to deceive the discriminator. The generator applies an encoder to extract low dimensional features from inputs which are used by the decoder as ingredients to craft a fake work. Somehow, the encoder and decoder are analogous to recipes for decomposition and synthesis, respectively. Hence, a generator learns unique recipes for the target class if it is trained purely using the samples from that class. Provided a sample from a different class, the generator will produce a pool forgery because of the wrong recipes used. In contrast, the discriminator aims to determine whether a given sample is genuine. It applies an independent encoder to explore major features of samples as the basis for judgement. These features can be treated as signatures that mark genuine and synthetic samples. Similar to the generator, the discriminator cannot extract correct signatures unless input samples come from the target class. In this case, GANs are highly effective in recognizing patterns of different classes [19].

The proposed network applies two GANs in parallel, one of which is responsible for learning patterns of normal samples

(GAN_{normal}) and the other is for icing samples (GAN_{icing}). Two GANs share the same structure as shown in Fig 3. They are expressed as follows:

TABLE I
NETWORK ARCHITECTURE OF GAN

Layer	Output size (F/Ks/S) ¹
GeneratorEncoder	
Input	1x1x28
Conv (LeakyReLU/Batchnorm)	4x1x25(4/4/1)
Conv	8x1x22(8/4/1)
GeneratorDecoder	
ConvTran (LeakyReLU/Batchnorm)	8x1x25 (8/4/1)
ConvTran (LeakyReLU/Batchnorm)	1x1x28 (1/4/1)
Tanh	1x1x28
Discriminator	
Input	1x1x28
Conv (LeakyReLU/Batchnorm)	4x1x25(4/4/1)
Conv	8x1x22(8/4/1)
FC	1
Sigmoid	1

¹ Filters/Kernel size/Stride

$$\begin{aligned}
 h_{ge}^i &= GE_i(x) \\
 x_{gd}^i &= GD_i(h_{ge}^i) \\
 h_{de}^i &= DE_i(x_{gd}^i) \\
 y^i &= h_{de}^i - h_{ge}^i
 \end{aligned} \tag{2}$$

where $i \in \{n, ic\}$ denotes normal and icing cases, respectively. $GE(\cdot)$, $GD(\cdot)$ and $DE(\cdot)$ present encoders and decoders in the generator and discriminator, respectively. $x_{gd}^i \in \mathcal{R}^{1 \times 28}$ is the synthetic sample. $h_{ge}^i \in \mathcal{R}^{8 \times 1 \times 22}$ and $h_{de}^i \in \mathcal{R}^{8 \times 1 \times 22}$ are extracted features of original and synthetic samples, respectively. $y^i \in \mathcal{R}^{8 \times 1 \times 22}$ are outputs of GANs. The detailed structure of GANs can be found in Table I.

Output y^i is a tensor composed of feature differences between original and synthetic samples. All outputs of two GANs are passed to the concatenation layer $CON(\cdot, \cdot)$ shown in Fig 4. This layer combines y^i to produce 8 channels of 2×22 matrices F :

$$F(i, :, :) = [y^n(i, :, :); y^{ic}(i, :, :)], 1 \leq i \leq 8. \tag{3}$$

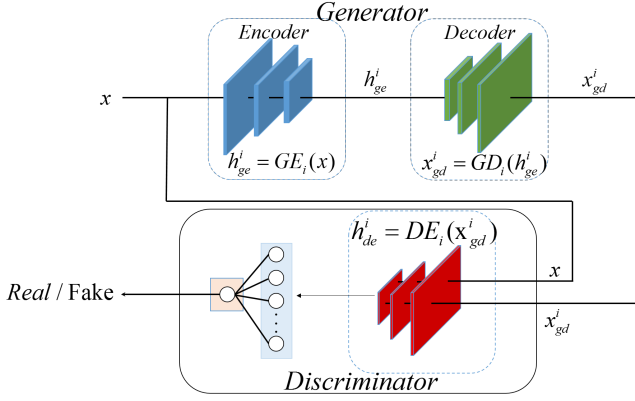


Fig. 3. The structure of GANs

where i denotes the index for channels. The spacial information of concatenated outputs contains important patterns of inputs that are essential for classification.

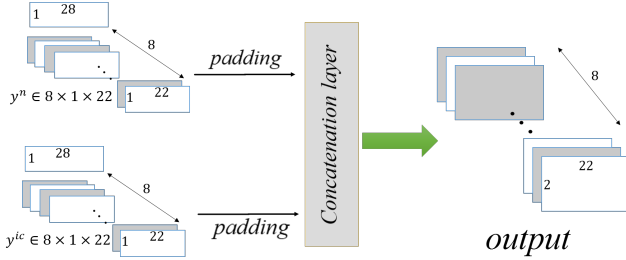


Fig. 4. The structure of concatenation layer

CNNs are well-known by its power to explore spatial information of samples [38], [32], [28]. The characteristics of inputs are decomposed layer-by-layer through the network where each layer is focused on learning a particular type of features. To classify the states of wind turbine blade, concatenated signals F are passed to the CNN classifier for anomaly detection:

$$Y = CNN(F) \quad (4)$$

where $Y \in \mathcal{R}^{1 \times 2}$ is a vector whose elements present probabilities of normal and abnormal icing classes. The detailed structure of the CNN is introduced in Table II.

TABLE II
NETWORK ARCHITECTURE OF CNN

Layer	Output size (F/Ks/S) ¹
Input	8x2x22
Conv2d (LeakyReLU/Batchnorm)	4x2x19(4/(1,4)/(1,1))
FC	2
Softmax	2

¹ Filters/Kernel size/Stride

To conclude, the proposed network in (1) can be further expanded as:

$$Y = CNN \{CON [GAN_n(x), GAN_{ic}(x)]\} \quad (5)$$

2) *Training procedure*: As the generator and the discriminator of a GAN are constructed with opposite purposes, they are

updated in turn based on the game theory. In each iteration, one part remains unchanged whilst the other is updated to optimize current strategies against its opponent. The whole procedure advances until the Nash equilibrium is achieved. In the end, both parts learn their optimal strategies and reach a balance [14].

Given a batch of samples, the optimization criteria for the generator and the discriminator are described as follows [19]:

Generator G_i :

$$\min L_{G_i}(x)$$

s.t.

$$L_{G_i}(x) = \omega_c * L_{con}(x) + \omega_a * L_{adv}(x) + \omega_f * L_f(x)$$

$$L_{con}(x) = \frac{1}{N_i} \sum_{j=1}^{N_i} \|x_j^i - G_i(x_j^i)\|_2$$

$$L_{adv}(x) = \frac{1}{N_i} \sum_{j=1}^{N_i} \log(1 - D_i(G_i(x_j^i)))$$

$$L_f(x) = \frac{1}{N_i} \sum_{j=1}^{N_i} \|GE_i(x_j^i) - DE_i(G_i(x_j^i))\|_2$$

Discriminator D_i :

$$\min L_{D_i}(x)$$

s.t.

$$L_D(x) = \frac{1}{N_i} \sum_{j=1}^{N_i} [\log D_i(x_j^i) + \log(1 - D_i(G_i(x_j^i)))] \quad (6)$$

where $i \in \{n, ic\}$ denotes severity cases, N_i is the batch size of class i and $x_j^i \in \mathcal{R}^{1 \times 28}$ presents the j th sample of class i .

In the next step, training samples are propagated forward through the pre-trained GANs and the outputs are passed to the concatenation layer to generate feature tensors F for classification.

As a classification problem, the cross-entropy loss is applied as the optimization criterion:

$$\min L_{CNN}(F)$$

s.t.

$$L_{CNN}(F) = \sum_i \frac{1}{N_i} \sum_{j=1}^{N_i} -\log(CNN(F_j^i)) \quad (7)$$

where F_j^i represents the feature tensor of the j th sample in class i . Unlike GANs, samples of normal and icing classes are used to train the CNN at the same time.

B. PGANT: non-sufficient labeled data scenario

Enough high-quality labeled data is usually difficult to acquire, especially for industrial scenarios, not only because retrofitting enough sensors in packaged equipment is sometimes challenging, but also expensive and laborious labeling makes it daunting. For above reasons, transfer learning is increasingly becoming a promising tool to solve the basic problem of unlabeled and insufficient data under various operating conditions, through utilizing the model trained on

data from source domain to improve learning performance of target domain.

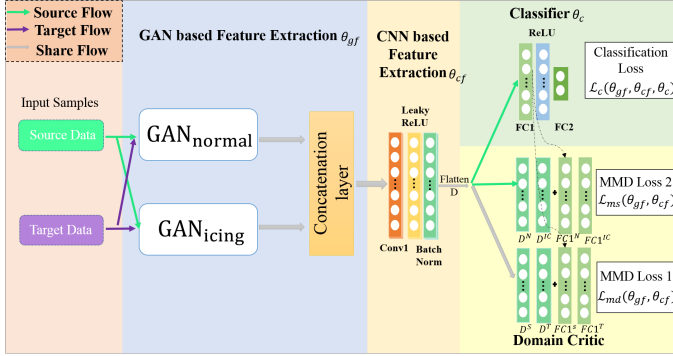


Fig. 5. The structure

1) *Method overview*: The neural network designed for icing detection of wind turbine blade without enough labeled data is composed of two GANs in parallel following by a classifier and a domain critic as shown in Fig 5. The structures of two GANs and concatenation layer in this part are as the same as those in section III-A.

We define a source domain dataset $x^s = \{x_i^s\}_{i=1}^{N^s}$ with labels $y^s = \{y_i^s\}_{i=1}^{N^s}$, a target domain dataset $x^t = \{x_i^t\}_{i=1}^{N^t}$. Usually the feature space in source domain and target domain are the same ($x^s, x^t \in \chi$) but $P(x^s) \neq P(x^t)$, where $P(\cdot)$ represents a marginal probability distribution. In most cases, source domain samples are sufficient enough to learn an accurate classifier and with much larger data size than the target domain, which means $N^s \gg N^t$.

There are four parts in our transfer learning framework, GAN based feature extractor, CNN based feature extractor, followed by classifier and domain critic. In the training stage, we first train GAN_{normal} and GAN_{icing} using normal and icing samples independently, and then initialize the two GANs in our proposed framework with the trained parameters. After concatenation layer, features F extracted from GAN based neural networks are passed to CNN based feature extractor for further feature exploring: $D = cnn(F)$. As shown in Fig 5, the CNN based feature extractor includes three layers: a convolution layer, a LeakyReLU activation layer, and a BatchNorm layer. For source domain data, a fully collected network is used to classify the feature vectors extracted through CNN based neural networks: $Y = FNN(D)$. In our proposed framework, the domain adaptation module includes a source-target domain distribution discrepancy and a normal-icing domain distribution discrepancy.

For a given input x^s and x^t , the feed forward path can be summarized through the following equations,

$$\begin{aligned} y_s^n &= GAN_{normal}(x^s), & y_t^n &= GAN_{normal}(x^t) \\ y_s^{ic} &= GAN_{icing}(x^s), & y_t^{ic} &= GAN_{icing}(x^t) \\ F_s &= [y_s^n; y_s^{ic}], & F_t &= [y_t^n; y_t^{ic}] \\ D_s &= cnn(F_s), & D_t &= cnn(F_t) \\ Y_s &= FNN(D_s) \end{aligned}$$

2) *Training procedure*: The proposed transfer learning framework has the following three optimization objects.

- 1) minimize the classification error in the source domain dataset;
- 2) minimize the MMD distance between the source and target domain dataset;
- 3) maximize the MMD distance between the normal and icing samples in source domain dataset.

1) *Object1*: In order to accomplish transfer icing detection, our proposed framework should be able to distinguish icing cases from normal cases and learn domain-invariant features. Specifically, the classifier is designed to identify icing states. Therefore, the first optimization object is to minimize the classification error in the source domain dataset. To compute the difference between the predicted label \tilde{Y}_i and the ground truth Y_i in the source domain, binary cross entropy loss function \mathcal{L}_c is used to update the GAN based feature extractor, the CNN based feature extractor, and the classifier with parameters θ_{gf} , θ_{cf} and θ_c :

$$\mathcal{L}_c = -\frac{1}{N^s} \sum_{i=1}^{N^s} \sum_j^{|m,ic|} \mathbb{I}_{Y_i}(j) \log(\tilde{Y}_i(j)) \quad (8)$$

where, \mathbb{I}_{Y_i} is an indicator function for label Y_i .

2) *Object2*: The domain critic module is designed to learn not only the domain-invariant features between the source domain and target domain but also state-distinguished vectors between normal and icing samples of the source domain. To solve the distribution difference between the source and target domain, we utilize MMD to learn invariant feature representation. Furthermore, two feature vectors are taken into consideration, features from CNN based feature extraction and features from the first fully connected layer, to improve the performance of MMD learning. Therefore, the distribution discrepancy distance between features learned from different domain can be written as:

$$\begin{aligned} \mathcal{L}_{md} &= \left\| \frac{1}{N^s} \sum_{i=1}^{N^s} D_i^s - \frac{1}{N^t} \sum_{i=1}^{N^t} D_i^t \right\|_H^2 \\ &+ \left\| \frac{1}{N^s} \sum_{i=1}^{N^s} FC1_i^s - \frac{1}{N^t} \sum_{i=1}^{N^t} FC1_i^t \right\|_H^2 \end{aligned} \quad (9)$$

where N^T is the number of training samples from the target domain, and $\|\cdot\|_H$ is a reproducing kernel Hilbert space. In practical, we use the unbiased estimation based on the Gaussian radial basis function (RBF), i.e., $k(x, y) = \exp(-\|x - y\|^2 / 2\sigma^2)$ [36] to complete the MMD computation.

3) *Object3*: In our proposed network, state-distinguished vectors in source domain are learned not only by binary

cross entropy loss in classifier, but also through MMD loss in domain critic. The optimization object in this part is to maximize the distribution discrepancy distance between normal and icing cases in source domain:

$$\begin{aligned} \mathcal{L}_{ms} = & \left\| \frac{1}{N^N} \sum_{i=1}^{N^N} D_i^N - \frac{1}{N^{IC}} \sum_{i=1}^{N^{IC}} D_i^{IC} \right\|_H^2 \\ & + \left\| \frac{1}{N^N} \sum_{i=1}^{N^N} FC1_i^N - \frac{1}{N^{IC}} \sum_{i=1}^{N^{IC}} FC1_i^{IC} \right\|_H^2 \end{aligned} \quad (10)$$

where N^n is the number of normal samples from the source domain, and N^{IC} is the number of icing samples from the source domain.

Combining those three optimization objects, the final objective function can be expressed in terms of the binary cross entropy loss \mathcal{L}_c of the classifier according to Eq. 8 and the distribution discrepancy distance \mathcal{L}_{md} and \mathcal{L}_{ms} associated with MMD of domain critic, i.e:

$$\mathcal{L}(\theta_{gf}^*, \theta_{cf}^*, \theta_c^*) = \min_{\theta_{gf}, \theta_{cf}, \theta_c} (\mathcal{L}_c - \alpha \mathcal{L}_{ms} + \beta \mathcal{L}_{md}) \quad (11)$$

where the hyperparameters α and β determine how strong the domain critic is. As shown in Fig 5, θ_{gf} , θ_{cf} , and θ_c denote the parameters for GAN based feature extraction, CNN based feature extraction and classifier, respectively.

We train the proposed method by Adam algorithm [21], the parameters θ_{gf} , θ_{cf} , and θ_c are updated as follows:

$$\begin{aligned} \theta_{gf} & \leftarrow \theta_{gf} - \xi \left(\frac{\partial \mathcal{L}_c}{\partial \theta_{gf}} - \alpha \frac{\partial \mathcal{L}_{ms}}{\partial \theta_{gf}} + \beta \frac{\partial \mathcal{L}_{md}}{\partial \theta_{gf}} \right) \\ \theta_{cf} & \leftarrow \theta_{cf} - \xi \left(\frac{\partial \mathcal{L}_c}{\partial \theta_{cf}} - \alpha \frac{\partial \mathcal{L}_{ms}}{\partial \theta_{cf}} + \beta \frac{\partial \mathcal{L}_{md}}{\partial \theta_{cf}} \right) \\ \theta_c & \leftarrow \theta_c - \xi \frac{\partial \mathcal{L}_c}{\partial \theta_c} \end{aligned} \quad (12)$$

where ξ is the learning rate.

C. Two-Stage Training of Neural Networks

Normally, neural networks are trained as an entirety using all training data. Practically, this training scheme may encounter two problems. With a large number of model parameters, it is extremely difficult to select good initial values to start with, which highly influences the performance of trained models. Since all model parameters are updated simultaneously, the algorithm requires many epochs to converge. In addition, given a large dataset, it takes long iterations for each epoch to finish a complete data scan.

This paper proposes a two-stage training scheme in order to improve model performance and reduce computational costs. To begin with, the training data are partitioned into two parts: normal and icing. In the first stage of training, components with differing functionality in the neural network are trained independently using different parts of the data. By updating fewer variables and using less data per time, model parameters are well initialized and the total computational costs are effectively reduced. The second stage applies the pre-trained model in stage one as the basis and conducts a global optimization for the entire neural network so that the model performance can be further improved.

IV. EXPERIMENTS RESULTS AND COMPARISONS

A. Experiment Setup

1) *Dataset Description:* Thanks to the first Industrial Big Data Innovation Competition (the Competition) in 2017, we have access to the real data from a wind farm in China. The raw data is collected from the supervisory control and data acquisition (SCADA) system which includes hundreds of dimensions every 7 seconds. According to the engineers' domain-specific knowledge, 26 continuous variables including real-time environmental data and wind turbine operating data relevant to the icing detection are preserved as the given multivariate signals. Detailed description of these variables is available online [2].

We choose three wind turbines' monitoring data for validating the performance of our proposed intelligent icing detection frameworks. For each wind turbine, we have icing and normal samples based on the fault records. Due to commercial confidentiality, all data given in the Competition have been encrypted, thus they lost the physical meaning of the original data in real conditions. Data details of three wind turbines are presented in Table III.

We proposed two scenarios for GAN+CNN based framework and GAN+Transfer learning framework, respectively, they are (we split the dataset in Table IV):

- 1) 10% of icing samples from Turbine A ($A \in [15, 21, 08]$) and the same number of normal samples, which are randomly chosen, as the training set. 40% of icing samples from Turbine A and ten times than that from normal samples as the testing set;
- 2) 60% of icing samples from Turbine A and the same number of normal samples, which are randomly chosen with labels, as the source domain set. The same number of samples from Turbine B without labels as the target domain set. 40% of icing samples of Turbine B and ten times than that of normal samples as the testing set.

TABLE III
DATASET DETAILS

Turbine No.	WT 15	WT 21	WT 8
Total Samples	393886	190494	202328
Normal Samples	350255(88.9%)	168930(88.7%)	180596(89.3%)
Icing samples	23892(6.1%)	10638(5.6%)	11308(5.5%)
Invalid Samples	19739(5.0%)	10926(5.7%)	10424(5.2%)
Period	2015.11 and 2015.12	2015.11	2015.11

TABLE IV
EXPERIMENTS DESIGN

Experiments	Training dataset	Testing dataset
WT 15	Labeled 15: 10%	WT 15: 40%
WT 21	Labeled 21: 10%	WT 21: 40%
WT 8	Labeled 08: 10%	WT 8: 40%
WT 15 - WT 21	Labeled 15: 60% Unlabeled 21: 60%	WT 21: 40%
WT 15 - WT 8	Labeled 15: 60% Unlabeled 8: 60%	WT 8: 40%
WT 21 - WT 8	Labeled 21: 60% Unlabeled 8: 60%	WT 8: 40%

2) *Data Preprocessing*: Data quality is often of vital importance to the performance of the constructed model. A uniform data format after data processing makes subsequent model training more conveniently manipulated. In our paper, we preprocess the data as follows: invalid data elimination, data balancing, new primary features extraction, and data normalization.

About 5% of the data in each wind turbine is invalid as shown in Table III. They are unable to provide useful information and will have an adverse effect on the classification performance, so we directly eliminate them from the whole dataset. Besides, the number of normal samples is much more than that of icing samples, which makes our problem a typical case of imbalanced scenarios. When normal and icing labels are imbalanced, classifiers based on neural networks will ensure the accuracy of the majority classes by sacrificing the minority classes [40], which means the diagnostic results will bias towards normality for when testing. However, for icing detection in wind farms, our focus should be specifically on those minority icing classes. In this study, we adopt strong rule filter and down sampling to imbalance the dataset. The strong rule filter is that we only consider records where the wind power output is less than 2. Under the icing conditions, icing accretion on the wind turbines would cause changes of the blades surface airfoil, thus inevitably decreasing power coefficient and power output. Specifically, when a wind turbine blade is icing, it can not output relatively high power, which is consistent with the information we get from the three wind turbines: icing samples are almost impossible to appear under the condition when wind power output is more than 2.

After balancing our dataset, a primary feature engineering is applied to help describe the behavior of wind turbines and their operating environments. We first analyze the 26 variables selected by engineers in pairs. It can be found that because of the symmetrical mechanical structures of wind turbines, the pitch angle, pitch speed and motor temperature of three blades in one wind turbine at the same time are almost linear correlation. Therefore, we only consider the mean value of these three variables. We also notice that three ratios will show a growing trend during the icing period, which are added in the input variables:

$$\begin{aligned}\kappa_{w2p} &= \left(\frac{v_{ws} + 5}{p + 5}\right)^2 - 1 \\ \kappa_{w2g} &= \left(\frac{v_{ws} + 5}{v_{gs} + 5}\right)^2 - 1 \\ \kappa_{w2pg} &= (\kappa_{w2p} + 1)(\kappa_{w2gs} + 1) - 1\end{aligned}\quad (13)$$

where v_{ws}, p, v_{gs} represent wind speed, power, and generator speed, respectively.

According to the model of Ice accretion on structures proposed by Makkonen [26], wind speed and temperature are two important factors contributing to icing blades, of which the most direct effect is that the output power is relatively low at the same wind speed. Therefore, significant factors related to temperature and power should also be considered, which

are as follows:

$$\begin{aligned}\kappa_1 &= T_{int} - T_{env}, \quad \kappa_2 = \frac{p}{v_{gs}}, \quad \kappa_3 = \frac{p}{(v_{ws})^3} \\ \kappa_4 &= \frac{\kappa_2}{v_{ws}^2}, \quad \kappa_5 = \frac{v_{gs}}{v_{ws}}\end{aligned}\quad (14)$$

The detailed input variables are summarized in Table V

TABLE V
DETAILED ATTRIBUTES

Number	Name	Description
1	wind_speed	wind speed
2	generator_speed	generator speed
3	power	grid side active power
4	wind_direction	wind direction
5	wind_direction_mean	mean of wind direction every 25 seconds
6	yaw_position	yaw position
7	yaw_speed	yaw speed
8	acc_x	X-direction acceleration
9	acc_y	Y-direction acceleration
10	environment_tmp	environmental temperature
11	int_tmp	cabin temperature
12	pitch1_ng5_tmp	ng5 1 temperature
13	pitch2_ng5_tmp	ng5 2 temperature
14	pitch3_ng5_tmp	ng5 3 temperature
15	pitch1_ng5_DC	ng5 1 charger DC current
16	pitch2_ng5_DC	ng5 2 charger DC current
17	pitch3_ng5_DC	ng5 3 charger DC current
18	pitch_angle_mean	mean pitch angle of three blades
19	pitch_speed_mean	mean pitch speed of three blades
20	pitch_moto_tmp_mean	mean pitch motor temperature of three blades
21	κ_{w2p}	ratio 1 showing growing trend during icing period
22	κ_{w2g}	ratio 2 showing growing trend during icing period
23	κ_{w2pg}	ratio 3 showing growing trend during icing period
24	κ_1	temperature difference between environment and cabin
25	κ_2	torque
26	κ_3	power coefficient
27	κ_4	thrust coefficient
28	κ_5	ratio between generator speed and wind speed

Thereafter, data normalization is conducted to eliminate the large magnitude difference between different variables without changing their distributions and interdependence. This can also speed up the learning efficiency of subsequent models. In this study, the following formula was used.

$$\tilde{x} = y_{min} + (y_{max} - y_{min}) * \frac{x - x_{min}}{x_{max} - x_{min}} \quad (15)$$

where x and \tilde{x} correspond to data before and after normalization, respectively, x_{max} and x_{min} correspond to the maximum and minimum values of the raw data, and y_{max} and y_{min} are the maximum and minimum values of the target range for the raw data. The target value of normalization in our paper is selected as $[-1, 1]$ owing to the value range of the activation function tanh is $[-1, 1]$.

3) *Evaluation Criteria*: Because there are much more normal samples than abnormal icing samples in our case, accuracy is not enough to measure the model performance. The overall performance will be compared by using the area under curve (AUC) of the receiver operating characteristic (ROC). In ROC,

the true positive rate (TPR) is as a function of the false positive rate (FPR). TPR and FPR are defined as follows,

$$\begin{aligned} TPR &= \frac{TP}{TP + FN} \\ FPR &= \frac{FP}{FP + TN} \end{aligned} \quad (16)$$

where TP is the number of positive samples predicted to be positive. FN is the number of positive samples predicted to be negative. FP is the number of negative samples predicted to be positive, and TN is the number of negative samples predicted to be negative. AUC (the range is $[0, 1]$) is not affected by class distribution, which is suitable for data sets with imbalanced class distribution.

We also notice that engineers and maintainers are more concerned about the icing cases in real applications. That means they are more tolerant of false positives compared with false negatives. Therefore, we also consider a new score (utilized in the Competition) to help evaluate our proposed models:

$$S = 1 - \alpha * \frac{FN}{N_{normal}} - (1 - \alpha) * \frac{FP}{N_{fault}} \quad (17)$$

where $\alpha = \frac{N_{fault}}{N_{normal}}$. The range of S is $[0, 1]$. The value is more close to 1, the better performance the model is.

B. Experimental Analysis

1) *PGANC Icing Diagnosis*: For comparing the performance of our proposed PGANC diagnosis framework, we consider the other two methods:

- 1) **SVC**: Traditional machine learning method SVC is used for comparison;
- 2) **CNN-based network**: To present ablation analysis of two GAN-based networks in our proposed network, we substitute them with a CNN-based network, and applied it on the data analysis of three wind turbines. The average result of 5 random initialization was taken as the final result.

Results corresponding to this experiment is shown in Table VI. From this table, we can see that our proposed two-stage PGANC framework outperforms all other methods. GAN-based networks get better performance means that GAN is better to capture intrinsic features in different classes (normal and icing cases in our paper) than CNN. One phenomenon noticed here is that stage 2 whole training performs better than stage 1 step training.

TABLE VI
COMPARISON

Method	15		21		8	
	Score	AUC	Score	AUC	Score	AUC
SVC	0.840	0.888	0.915	0.931	0.860	0.897
CNN	0.839	0.882	0.904	0.919	0.869	0.880
PGANC stage1	0.776	0.864	0.836	0.883	0.830	0.848
PGANC stage2	0.884	0.908	0.926	0.940	0.915	0.933

TABLE VII
COMPARISON2, TRAINING 5%, TESTING 5:1

Method	15		21		8	
	Score	AUC	Score	AUC	Score	AUC
SVC	0.859	0.884	0.925	0.944	0.903	0.923
CNN	0.863	0.884	0.900	0.927	0.909	0.926
PGANC stage1	0.811	0.851	0.871	0.904	0.851	0.878
PGANC stage2	0.876	0.896	0.924	0.943	0.945	0.949

2) *PGANT Icing Diagnosis*: For comparing the performance of our proposed PGANT diagnosis framework, we consider KNN, SVC, XGBOOST, PGANC diagnosis network. In this experiment, above methods are trained using labeled source domain data, and tested on target domain data.

Results corresponding to this experiment is shown in Table VIII. From this table, we can see that the performance of our proposed network is state-of-the-art in all comparing methods in terms of score evaluation. Although MCC of SVC and XGBOOST is sometimes show better performance, our proposed network is able to show comparing results. We should notice that PGANC network is also trained on source domain data, but it still gets better transfer performance on target domain data, which means that the GAN-based feature extraction not only captures our interesting characteristics in icing samples, but also show better generalization performance with higher robust ability given data from new turbines.

TABLE VIII
COMPARISON

Method	15-21		15-8		21-8	
	Score	AUC	Score	AUC	Score	AUC
KNN	0.401	0.659	0.341	0.595	0.487	0.656
SVC	0.676	0.810	0.629	0.739	0.770	0.810
XGBOOST	0.481	0.708	0.325	0.590	0.538	0.742
PGANC	0.715	0.823	0.654	0.723	0.805	0.815
PGANT	0.769	0.849	0.779	0.779	0.819	0.800

For comparing the performance of our proposed PGANT diagnosis framework, we also consider the ablation analysis of one addition MMD loss and GAN-based networks. In this part, we add Matthews Correlation Coefficient (MCC) [4] as one of our evaluation criteria, which can show whether the minority class could be predicted correctly from another perspective. The experiments are set as follows:

- 1) **GAN CNN+2 LOSS**: Method proposed in this paper;
- 2) **GAN CNN+1 LOSS**: In this method, all the networks are trained as described in Sec. III-B2, except trained without \mathcal{L}_{ms} ;
- 3) **CNN+2 LOSS**: In this method, GAN-based feature extraction is substituted by CNN-based networks and trained with two MMD loss \mathcal{L}_{ms} and \mathcal{L}_{md} .
- 4) **CNN+1 LOSS**: This framework is the same as **CNN+2 LOSS**, but trained without \mathcal{L}_{ms} .

We report the Evaluation Criteria averaged over five randomized trials. Results corresponding to this experiment is shown in Fig 6. From this figure, we can see that score and

AUC outperform other methods, but for MCC PGANC with one MMD loss gets better performance.

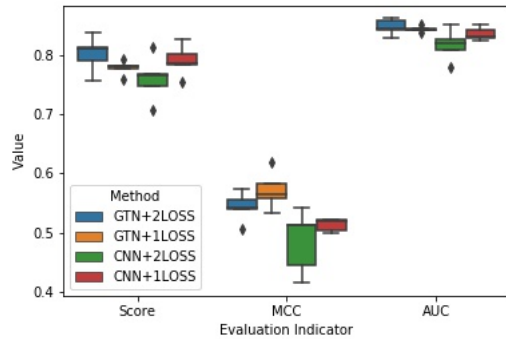


Fig. 6. Comparisons for the ablation study

V. CONCLUSION

To achieve intelligent icing diagnosis of wind turbine, we proposed PGANC and PGANT for sufficient and non-sufficient labeled data of target turbines, respectively. Two parallel GANs are used for distinguished feature capture of icing and normal samples, and two-stage training process is adopted to further improve training efficiency and performance. Our proposed methods are tested on real SCADA data from a wind farm. Because icing cases of wind turbines are much fewer than normal cases, we take MCC, AUC, and a score which focuses more on the false negative rate than the false positive rate as evaluation criteria. Empirical results show that 1) PGANC outperforms traditional CNNs, and PGANT achieves higher robustness for icing diagnosis for different wind turbines. 2) our proposed two-stage training contributes to higher accuracy and efficiency.

REFERENCES

- [1] British standards institution. overhead transmission lines-design criteria. iec 60826: 2017. Available at: <https://webstore.ansi.org/Standards/BSI/BSIEC608262017> (Accessed on 19 December 2020).
- [2] Detailed description for scada variables of wind turbines. Available at: <http://www.industrial-bigdata.com/Title>, (Accessed December 10, 2020).
- [3] The gan zoo: A list of all named gans. Available at: <https://github.com/hindupuravinash/the-gan-zoo> (Accessed: 13th December, 2020).
- [4] Alex Alexandridis, Eva Chondrodima, Georgia Paivana, Marios Stogianos, Elias Zois, and Haralambos Sarimveis. Music genre classification using radial basis function networks and particle swarm optimization. In *2014 6th Computer Science and Electronic Engineering Conference (CEECE)*, pages 35–40. IEEE, 2014.
- [5] Lorenzo Battisti. *Wind turbines in cold climates: Icing impacts and mitigation systems*. Springer, 2015.
- [6] Mengnan Cao, Yingning Qiu, Yanhui Feng, Hao Wang, and Dan Li. Study of wind turbine fault diagnosis based on unscented kalman filter and scada data. *Energies*, 9(10):847, 2016.
- [7] Siyuan Chen, Yuquan Meng, Haichuan Tang, Yin Tian, Niao He, and Chenhui Shao. Robust deep learning-based diagnosis of mixed faults in rotating machinery. *IEEE/ASME Transactions on Mechatronics*, 25(5):2167–2176, 2020.
- [8] Cheng Cheng, Beitong Zhou, Guijun Ma, Dongrui Wu, and Ye Yuan. Wasserstein distance based deep adversarial transfer learning for intelligent fault diagnosis. *arXiv preprint arXiv:1903.06753*, 2019.
- [9] Juchuan Dai, Wenxian Yang, Junwei Cao, Deshun Liu, and Xing Long. Ageing assessment of a wind turbine over time by interpreting wind farm scada data. *Renewable Energy*, 116:199–208, 2018.
- [10] Phong B Dao, Wieslaw J Staszewski, Tomasz Barszcz, and Tadeusz Uhl. Condition monitoring and fault detection in wind turbines based on cointegration analysis of scada data. *Renewable Energy*, 116:107–122, 2018.
- [11] Xinghui Dong, Di Gao, Jia Li, Zhang Jincan, and Kai Zheng. Blades icing identification model of wind turbines based on scada data. *Renewable Energy*, 162:575–586, 2020.
- [12] Sudhakar Gantasala, Jean-Claude Luneno, and Jan-Olov Aidanpää. Influence of icing on the modal behavior of wind turbine blades. *Energies*, 9(11):862, 2016.
- [13] Yiping Gao, Liang Gao, Xinyu Li, and Xuguo Yan. A semi-supervised convolutional neural network-based method for steel surface defect recognition. *Robotics and Computer-Integrated Manufacturing*, 61:101825, 2020.
- [14] Ian Goodfellow, Jean Pouget-Abadie, Mehdi Mirza, Bing Xu, David Warde-Farley, Sherjil Ozair, Aaron Courville, and Yoshua Bengio. Generative adversarial nets. In *Advances in Neural Information Processing Systems*, pages 2672–2680, 2014.
- [15] Arthur Gretton, Karsten M Borgwardt, Malte J Rasch, Bernhard Schölkopf, and Alexander Smola. A kernel two-sample test. *The Journal of Machine Learning Research*, 13(1):723–773, 2012.
- [16] Hamed Habibi, Ian Howard, and Silvio Simani. Reliability improvement of wind turbine power generation using model-based fault detection and fault tolerant control: A review. *Renewable Energy*, 135:877–896, 2019.
- [17] Yiqiang Han, Jose Palacios, and Sven Schmitz. Scaled ice accretion experiments on a rotating wind turbine blade. *Journal of Wind Engineering and Industrial Aerodynamics*, 109:55–67, 2012.
- [18] Matthew C Homola, Per J Nicklasson, and Per A Sundsbø. Ice sensors for wind turbines. *Cold regions science and technology*, 46(2):125–131, 2006.
- [19] Wenqian Jiang, Yang Hong, Beitong Zhou, Xin He, and Cheng Cheng. A gan-based anomaly detection approach for imbalanced industrial time series. *IEEE Access*, 7:143608–143619, 2019.
- [20] Asifullah Khan, Anabia Sohail, Umme Zahoor, and Aqsa Saeed Qureshi. A survey of the recent architectures of deep convolutional neural networks. *arXiv preprint arXiv:1901.06032*, 2019.
- [21] Diederik P Kingma and Jimmy Ba. Adam: A method for stochastic optimization. *arXiv preprint arXiv:1412.6980*, 2014.
- [22] Yann LeCun, Bernhard Boser, John Denker, Donnie Henderson, R Howard, Wayne Hubbard, and Lawrence Jackel. Handwritten digit recognition with a back-propagation network. *Advances in neural information processing systems*, 2:396–404, 1989.
- [23] Yann LeCun, Bernhard Boser, John S Denker, Donnie Henderson, Richard E Howard, Wayne Hubbard, and Lawrence D Jackel. Back-propagation applied to handwritten zip code recognition. *Neural computation*, 1(4):541–551, 1989.
- [24] Ruonan Liu, Guotao Meng, Boyuan Yang, Chuang Sun, and Xuefeng Chen. Dislocated time series convolutional neural architecture: An intelligent fault diagnosis approach for electric machine. *IEEE Transactions on Industrial Informatics*, 13(3):1310–1320, 2016.
- [25] Mingsheng Long, Yue Cao, Jianmin Wang, and Michael Jordan. Learning transferable features with deep adaptation networks. In *International conference on machine learning*, pages 97–105. PMLR, 2015.
- [26] Lasse Makkonen. Models for the growth of rime, glaze, icicles and wet snow on structures. *Philosophical Transactions of the Royal Society of London. Series A: Mathematical, Physical and Engineering Sciences*, 358(1776):2913–2939, 2000.
- [27] LI Ningbo, YAN Tao, LI Naipeng, KONG Detong, LIU Qingchao, and LEI Yaguo. Ice detection method by using scada data on wind turbine blades. *Power Generation Technology*, 39(1):58–62, 2018.
- [28] N. Passalis and A. Tefas. Training lightweight deep convolutional neural networks using bag-of-features pooling. *IEEE Transactions on Neural Networks and Learning Systems*, 30(6):1705–1715, 2019.
- [29] Patrick Rizk, Nawal Al Saleh, Rafic Younes, Adrian Ilinca, and Jihan Khoder. Hyperspectral imaging applied for the detection of wind turbine blade damage and icing. *Remote Sensing Applications: Society and Environment*, 18:100291, 2020.
- [30] Andrew M Saxe, Pang Wei Koh, Zhenghao Chen, Maneesh Bhand, Bipin Suresh, and Andrew Y Ng. On random weights and unsupervised feature learning. In *ICML*, volume 2, page 6, 2011.
- [31] Dino Sejdinovic, Bharath Sriperumbudur, Arthur Gretton, and Kenji Fukumizu. Equivalence of distance-based and rkhs-based statistics in hypothesis testing. *The Annals of Statistics*, pages 2263–2291, 2013.

- [32] G. Shomron and U. Weiser. Spatial correlation and value prediction in convolutional neural networks. *IEEE Computer Architecture Letters*, 18(1):10–13, 2019.
- [33] L. Shu, X. Ren, Q. Hu, X. Jiang, J. Liang, G. Qiu, and HT Li. Influences of environmental parameters on icing characteristics and output power of small wind turbine. *Proc. CSEE*, 36(11):5873–5878, 2016.
- [34] Georgios Alexandros Skrimpas, Karolina Kleani, Nenad Mijatovic, Christian Walsted Sweeney, Bogi Bech Jensen, and Joachim Holboell. Detection of icing on wind turbine blades by means of vibration and power curve analysis. *Wind Energy*, 19(10):1819–1832, 2016.
- [35] Jannis Tautz-Weinert and Simon J Watson. Using scada data for wind turbine condition monitoring—a review. *IET Renewable Power Generation*, 11(4):382–394, 2016.
- [36] Eric Tzeng, Judy Hoffman, Ning Zhang, Kate Saenko, and Trevor Darrell. Deep domain confusion: Maximizing for domain invariance. *arXiv preprint arXiv:1412.3474*, 2014.
- [37] J. Wang, S. Li, B. Han, Z. An, H. Bao, and S. Ji. Generalization of deep neural networks for imbalanced fault classification of machinery using generative adversarial networks. *IEEE Access*, 7:111168–111180, 2019.
- [38] R. Xin, J. Zhang, and Y. Shao. Complex network classification with convolutional neural network. *Tsinghua Science and Technology*, 25(4):447–457, 2020.
- [39] W. Yang, C. Hui, Z. Chen, J. Xue, and Q. Liao. Fv-gan: Finger vein representation using generative adversarial networks. *IEEE Transactions on Information Forensics and Security*, 14(9):2512–2524, 2019.
- [40] Hua Yin and Keke Gai. An empirical study on preprocessing high-dimensional class-imbalanced data for classification. In *2015 IEEE 17th International Conference on High Performance Computing and Communications, 2015 IEEE 7th International Symposium on Cyberspace Safety and Security, and 2015 IEEE 12th International Conference on Embedded Software and Systems*, pages 1314–1319. IEEE, 2015.
- [41] Mengyao Yu, Sheng Fu, Yinbo Gao, Hao Zheng, and Yonggang Xu. Crack detection of fan blade based on natural frequencies. *International Journal of Rotating Machinery*, 2018, 2018.
- [42] Shiqi Yu, Rijun Liao, Weizhi An, Haifeng Chen, Edel B. García, Yongzhen Huang, and Norman Poh. Gaitganv2: Invariant gait feature extraction using generative adversarial networks. *Pattern Recognition*, 87:179 – 189, 2019.
- [43] Binhang Yuan, Chen Wang, Fei Jiang, Mingsheng Long, S Yu Philip, and Yuan Liu. Waveletfcnn: A deep time series classification model for wind turbine blade icing detection. 2019.
- [44] Lijun Zhang, Kai Liu, Yufeng Wang, and Zachary Bosire Omariba. Ice detection model of wind turbine blades based on random forest classifier. *Energies*, 11(10):2548, 2018.
- [45] M. Zhang, M. Gong, Y. Mao, J. Li, and Y. Wu. Unsupervised feature extraction in hyperspectral images based on wasserstein generative adversarial network. *IEEE Transactions on Geoscience and Remote Sensing*, 57(5):2669–2688, 2019.
- [46] Sufang Zhang. International competitiveness of china’s wind turbine manufacturing industry and implications for future development. *Renewable and Sustainable Energy Reviews*, 16(6):3903–3909, 2012.